A Numerical Analysis on Elastodynamic Dispersion Phenomena of Composite Pipes

Younho Cho*[†], Chong Myong Lee** and Joseph L. Rose**

Abstract An efficient technique for the calculation of guided wave dispersion curves in composite pipes is presented. The technique uses a forward-calculating variational calculus approach rather than the guess and iterate process required when using the more traditional partial wave superposition technique. The formulation of each method is outlined and compared. The forward-calculating formulation is used to develop finite element software for dispersion curve calculation. Finally, the technique is used to calculate dispersion curves for several structures, including an isotropic bar, two multi-layer composite bars, and a composite pipe.

Introduction

Composite tube and shaft structures are being used increasingly in a variety of weight-driven designs of critical structures, including automotive, aeronautical and aerospace applications (Rose, 1999; Achenbach, 1973; Lamb, 1917; Taeweel, et al., 2000; Rasttanawagcharoen and Datta, 1992; Bai, et al., 2002). Due to the high cost of composite materials and their high susceptibility to certain from events such as tool drops, effective, efficient methods of nondestructive evaluation (NDE) are crucial to maintaining the safety and integrity of these systems. One such NDE technique is the use of ultrasonic guided waves, which have the ability to rapidly detect defects at large distances (Rose, 1999).

One major hindrance to the use of ultrasonic guided waves in the NDE of composite shafts is the difficulty of efficiently calculating dispersion curves for these structures. Conventional methods of calculating dispersion curves fail for composite materials (Rose, 1999; Achenbach, 1973; Lamb, 1917; Taeweel et al., 2000). The necessary assumptions of isotropy, homogeneity, and a lossless medium do not hold for the Helmholtz decomposition, and the iterative process necessary for the partial wave superposition (PWS) technique becomes too cumbersome with the introduction of direction-dependent elastic constants. Therefore, the goal of the current effort is the development of a numerical method for the calculation of dispersion curves in composite tubes. To this end, a numerical study has been used to develop a computer package on guided wave propagation characteristics using the semi-analytical FEM technique in conjunction with the variational calculus formulation of the elastic energy induced by guided wave propagation in composites.

Mathematical Background

Mathematical formulation of the computational technique begins with the transformation of Navier's (differential) Equation of motion into an integral from using Hamilton's principle. Next, an assumption of time-harmonic wave excitation

is made and Fourier decomposition is performed on an arbitrary guided wave packet to produce a number of continuous, single-frequency sinusoids (Rose, 1999; Achenbach, 1973; Lamb, 1917; Taeweel, et al., 2000; Rasttanawagcharoen and Datta, 1992; Bai, et al., 2002, Charkraborty et al., 2002; Galan and Abascal, 2002). In this study, the guided wave propagation of the time harmonic wave form with a single frequency is simulated as the expansion of the corresponding modal wave motion at a reference point in the pipe axial direction (the propagation direction) by multiplying the phase change of the time harmonic exponential function by the reference modal function. This effectively reduces the dimensionality of the system, dropping the axial component and leaving only information for material properties, fiber orientation, geometry, etc., at a given cross-section.

The integral governing equation of guided wave propagation is derived through the variational calculus technique (VCT) for the functional in terms of the energy terms induced by the wave motion. In other words, physically this procedure is associated with the one to find a wave field which minimizes the functional and consequently satisfies the original differential type governing equation. A numerical integration process is then used to calculate each energy term for the integral governing equation while imposing traction-free surface boundary conditions on the shaft, yielding the guided wave dispersion equation in matrix form (Rose, 1999 ; Achenbach, 1973).

Unlike a dispersion equation in matrix form derived through a conventional differential approach such as the Helmholtz decomposition or PWS, the matrix of the dispersion equations for the present study produce a skew-symmetric matrix. This leads to a significant advantage in root extraction since an iteration technique with a proper initial guess is no longer needed, even for a guided wave mode with complex wave number (evanescent modes). In this form, a forward root-search algorithm is sufficient for finding all possible guidedwave modes, both propagating and evanescent, without time consuming iteration. Consequently, the divergence problem in root search due to improper initial guess, normally a significant computational obstacle, is eliminated. Instead, the solution convergence and accuracy of the present technique rely on the cross-sectional mesh profile of the FEM grid. This method still produces error inherent to numerical integration

Table 1 Comparison of PWS and VCT formulation of dispersion curves

Step	Partial Wave Superposition	Variational Calculus Technique
1	Separation of Variables (w,t); $e^{i(kz-wt)}$	Separation of Variables (w,t); $e^{i(kz-wt)}$
2	Develop governing differential equation	Develop governing integral equation
3	Assume a vector displacement	Make energy assumption (scalar) for displacement
4	Use constitutive equations for stress	Impose displacement and external force conditions
5	Impose traction free boundary conditions	Derive stiffness matrices with F=0
6	Set up dispersion equations in terms of stress (derived from stress terms)	Set up dispersion equation using displacements (derived from general free vibration equation)
7	Produce a non-symmetric generalized matrix	Produce Hermitian complex matrix with conjugates
8	Solve using iteration—time consuming and requires good initial guess	Use typical eigenvalue solver—no iteration, no initial guess

techniques, but this error is less than that produced by differential methods like PWS. Once a solution has been obtained using VCT, its convergence must be checked by varying the mesh to optimize for accuracy and computational efficiency. Optimization was performed using "LAPAC," a commercially available eigenvalue solution for vibration problems.

Comparison of techniques

Table 1 gives a comparison between PWS and VCT methods of dispersion curve generation.

As discussed above, the VCT formulation is significantly more computationally efficient than PWS due to the skew-symmetry of the resulting wave-vector matrix; in effect, the VCT reduces the number of unknowns to be determined for the final solution as well as allowing for a more direct, non-iterative solution process.

Summarized Mathematical Expressions for Dispersion Curve Development

The following outlines the principal equations used in the development of dispersion curves by Helmholtz decomposition, PWS and VCT.

Differential Calculus Techniques

Helmholtz Decomposition

The Helmholtz decomposition breaks down wave displacement into two orthogonal components; it uses (scalar potential + vector potential) to represent overall wave displacement. Decomposing wave displacement into purely horizontal and vertical components requires assumptions of homogeneity, isotropy, and an elastic medium. The basic process for Helmholtz decomposition is as follows:

Begin with Navier's Equation for motion from elasticity theory:

$$(\lambda + 2\mu)\nabla\nabla \bullet \overline{U} - \mu\nabla \times \nabla \times \overline{U} = \rho\frac{\partial^2 \overline{U}}{\partial t^2} \qquad (1)$$

The decomposition (scalar + vector potential):

$$\overline{U} = \nabla\Phi + \nabla \times \overrightarrow{H}, \qquad \nabla \bullet \overrightarrow{H} = 0 \qquad (2)$$

This allows the separation of the governing equation into orthogonal components:

$$\nabla\left[(\lambda + 2\mu)\nabla^2\phi - \rho\frac{\partial^2\phi}{\partial t^2}\right] + \nabla\times\left[\mu\nabla^2 H - \rho\frac{\partial^2 H}{\partial t^2}\right] = 0 \qquad (3)$$

Orthogonality of components allows the G.E. to be separated into two separate components:

$$\nabla^2\phi = \frac{1}{C_L^2}\frac{\partial^2\phi}{\partial t^2}, \quad C_L^2 = \frac{\lambda + 2\mu}{\rho} \quad ;$$
$$\nabla^2 H = \frac{1}{C_T^2}\frac{\partial^2 H}{\partial t^2}, \quad C_T^2 = \frac{\mu}{\rho} \qquad (4)$$

Traction free boundary conditions are then applied on the surfaces of the structure:

$$\sigma_{31} = \sigma_{33} = 0 \quad at \quad x_3 = \pm d/2 = \pm h \qquad (5)$$

Generating a system of equations to be solved for the dispersion curves; for non-trivial solutions, the determinant of [A] must equal zero:

$$\begin{bmatrix} A_{11} & A_{12} & A_{13} & A_{14} \\ A_{21} & A_{22} & A_{23} & A_{24} \\ A_{31} & A_{32} & A_{33} & A_{34} \\ A_{41} & A_{42} & A_{43} & A_{44} \end{bmatrix}\begin{bmatrix} A_1 \\ A_2 \\ B_1 \\ B_2 \end{bmatrix} = \begin{bmatrix} 0 \\ 0 \\ 0 \\ 0 \end{bmatrix} \quad Det\begin{bmatrix} A_{11} & A_{12} & A_{13} & A_{14} \\ A_{21} & A_{22} & A_{23} & A_{24} \\ A_{31} & A_{32} & A_{33} & A_{34} \\ A_{41} & A_{42} & A_{43} & A_{44} \end{bmatrix} = 0 \qquad (6)$$

Partial wave superposition

PWS differs from the Helmholtz decomposition in that rather than breaking a wave into orthogonal displacement components; it sums waves of all polarizations and determines wave modes through interference analysis. PWS is typically used for anisotropic, inhomogeneous media.

Formulation is based on decomposing a traveling wave into six components—upward and downward traveling longitudinal, shear horizontal, and shear vertical components:

$$U_i = \alpha_i \exp[ik(x + l_z z)]\exp[-i\omega t], \quad i = 1 \sim 6 \qquad (7)$$

Variational Calculus Technique

As discussed above, the VCT is based on a calculation of total wave energy rather than

displacement components. The mathematical process of this technique is as follows:

Lagrangian and Hamilton's principle:

$$\delta \int_{t_0}^{t_1} \{T - (U + V_E)\} dt = 0 \quad \text{(8)}$$

Where the kinetic energy is given by:

$$T = \frac{1}{2} \iiint_B \dot{u}^T \rho \dot{u} \, d(vol) \quad \text{(9)}$$

By Hooke's Law, the strain energy is:

$$U = \frac{1}{2} \iiint_B \varepsilon^T C \varepsilon \, d(vol) \quad \text{(10)}$$

The potential energy of the material is then:

$$V_E = -\int\int u^T \sigma_f \, d(surf) \quad \text{(11)}$$

Taking the Hamiltonian over a local element on the cross-sectional FEM model of composite pipe,

$$\Pi(x,y,z) = \frac{1}{2} \left[\kappa^2 k_2(x,y) + \kappa k_1(x,y) + k_0(x,y) - \omega^2 \mu(x,y) \right] \quad \text{(12)}$$

the dispersion equation of guided wave propagation along a composite pipe becomes:

$$\left(\kappa^2 [K_2] + \kappa [K_1] + [K_0] - \omega^2 [M] \right)\{U\} = \{0\} \quad \text{(13)}$$

$$AV = \kappa BV \qquad Det[A - \kappa B] = 0$$

Where,

$$V = \begin{bmatrix} U_0 \\ \kappa U_0 \end{bmatrix} \qquad A = \begin{bmatrix} \cdot & K_3 - \omega^2 M \\ K_3 - \omega M & K_2 \end{bmatrix}$$

$$B = \begin{bmatrix} K_3 - \omega^2 M & \cdot \\ \cdot & K_1 \end{bmatrix}$$

Patch Test Results for Code Verification

Several examples of VCT generation of frequency versus wave number dispersion curves are presented below. Each has been verified with benchmarking data from its corresponding reference.

Isotropic Bar

The isotropic bar results presented have been verified using (Taeweel, et al., 2000). The bar has a height to width ratio (H/W) of ½ and a Poisson's ratio of 0.4. Sixty four elements were used. Geometry is shown in Figure 1; the resulting dispersion curves are in Figure 2.
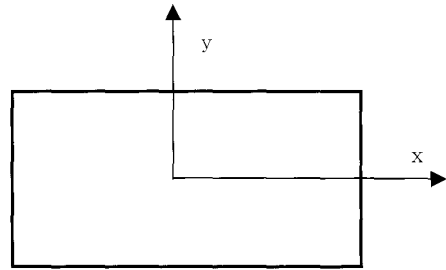

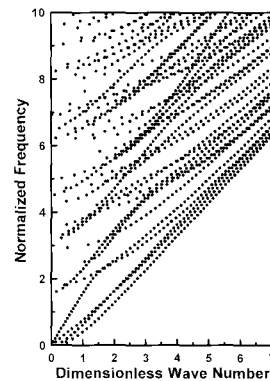Figure 1   Geometry of isotropic bar specimen

Figure 2   Wave number dispersion curves for isotropic bar

Layered Composite Bars

Below are two examples of layered composite bars, also from (Achenbach, 1973). The first case, presented in Figures 3 and 4 is a two-layered structure modeled with 48 elements. Figures 5 and 6 show geometry and results for a three layered structure, modeled using 64 elements. Both structures have ±30° fiber orientations, H/W = ½, and identical material properties, which are provided in Table 2.

Table 2   Material properties of layered composite bar specimens

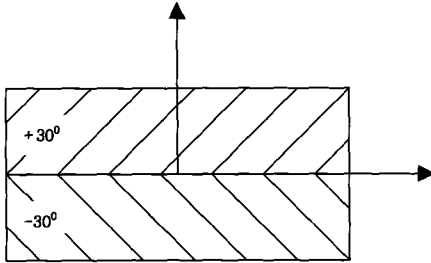|	E_L (GPa)	E_T (GPa)	G_{LT} (GPA)	G_{TT} (GPA)	$\upsilon_{LT} = \upsilon_{TT}$
2-Layer Bar	139.274	15.167	5.861	6.268	0.21
3-Layer Bar	139.274	15.167	5.861	6.268	0.21

Figure 3   Geometry of two layer composite bar
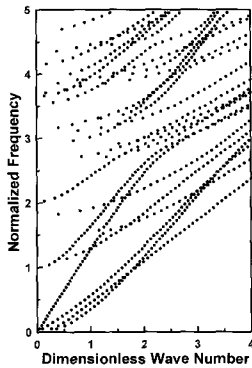
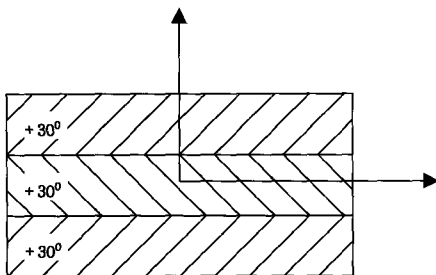Figure 4   Wave number dispersion curves for two-layer composite bar
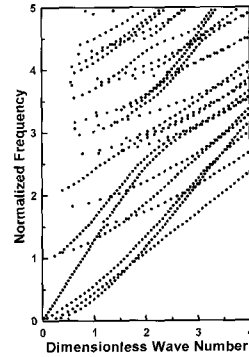

Figure 5   Geometry for three layer composite bar

Figure 6   Wave number dispersion curves for three layer composite bar

Layered Composite Pipe

Finally, results are presented below for a composite pipe specimen. The structure modeled had two plies of graphite/epoxy with a layup of [0/90], an inside diameter of 9.5 inches and an outside diameter of 10 inches. In this case, two models iterations were made, the first with 120 elements and the second with 240. Layup and element configuration is shown in Figure 7, material properties are shown in Table 3, and Figures 8 and 9 show the 120 and 240 element model results, respectively. In this case, phase velocity dispersion curves are presented.
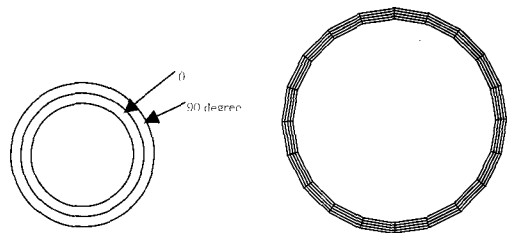

Figure 7   Layup and element setup for composite pipe model

Table 3   Material properties of composite pipe structure

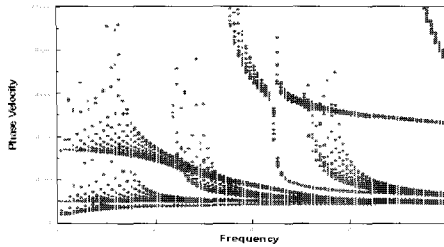|	C_{11} (GPa)	C_{12} (GPa)	C_{13} (GPa)	C_{33} (GPa)	C_{44} (GPa)	ρ (g/cm³)
0°	13.92	6.92	6.44	160.73	7.07	1.8
90°	13.92	6.44	6.92	13.92	7.07	1.8

Figure 9 Phase velocity dispersion curves for composite pipe from 120 element model
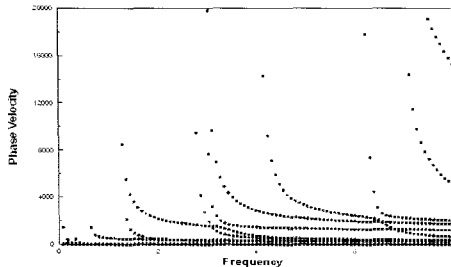

Figure 10 Phase velocity dispersion curves for composite pipe from 240 element model

From Figures 9 and 10, it is important to note the significant improvement in convergence resulting from increasing the number of elements. Additionally, note that in several locations, particularly at lower frequencies, multiple modes appear to be present at closely grouped frequencies where the 120 element model lacked the resolution to make such a distinction.

Concluding Remarks

A numerical approach based on the hybrid FEM technique for dispersion curve analysis of composite structures is introduced. The present method can be applied to a wide range of guided wave problems providing a new theoretical scheme to overcome the technical limitations of conventional pure theoretical methods due to either material anisotropy or geometrical complexity. It is expected that the present results can be a useful physical guideline for guided wave mode tuning and signal analysis in composite health monitoring.

References

Rose, J. L. (1999) *Ultrasonic Waves in Solid Media*, Cambridge University Press, Cambridge

Achenbach, J. D. (1973) *Wave Propagation in Elastic Solids*, New York: North-Holland

Lamb H. (1917) Waves in an Elastic Plate, P. Roy. Soc. Lond. A Mat., Vol. 93, pp. 114-128

Taeweel, H., Dong, S. B. and Kazic, M. (2000) Wave Reflection from the Free End of a Cylinder with an Arbitrary Cross-Section, International Journal of Solids and Structures, Vol. 37, pp. 1701-1726

Rattanawangcharoen, N. and Datta, A. H. (1992) Wave Propagation in Laminated Composite Circular Cylinders, *International Journal of Solids and Structures*, Vol. 29, No. 6, pp. 767-781

Bai, H. Shah, A. H., Popplewell, N. and Datta, S. K. (2002) Scattering of Guided Waves by Circumferential Cracks in Composite Cylinders, *International Journal of Solids and Structures*, 4583-4603

Chakraborty, A., Mahapatra, D. Roy and Gopalakrishnan, S. (2002) Finite Element Analysis of Free Vibration and Wave Propagation in Asymmetric Composite Beams with Structural Discontinuities, *Composite Structures*, Vol. 55, pp. 23-36

Galan, J. M. and Abascal, R. (2002) Numerical Simulation of Lamb Wave Scattering in Semi-Infinite Plates, *International Journal for Numerical Methods in Engineering*, Vol. 53, pp. 1145-1173